



Endocrine regulation of multichromatic color vision

Robert D. Mackin^a, Ruth A. Frey^a, Carmina Gutierrez^a, Ashley A. Farre^a, Shoji Kawamura^b, Diana M. Mitchell^a, and Deborah L. Stenkamp^{a,1}

^aDepartment of Biological Sciences, University of Idaho, Moscow, ID 83844; and ^bDepartment of Integrated Biosciences, University of Tokyo, 277-0882 Kashiwa, Japan

Edited by Robert Johnston, The Johns Hopkins University, Baltimore, MD, and accepted by Editorial Board Member Jeremy Nathans July 8, 2019 (received for review March 25, 2019)

Vertebrate color vision requires spectrally selective opsin-based pigments, expressed in distinct cone photoreceptor populations. In primates and in fish, spectrally divergent opsin genes may reside in head-to-tail tandem arrays. Mechanisms underlying differential expression from such arrays have not been fully elucidated. Regulation of human red (*LWS*) vs. green (*MWS*) opsins is considered a stochastic event, whereby upstream enhancers associate randomly with promoters of the proximal or distal gene, and one of these associations becomes permanent. We demonstrate that, distinct from this stochastic model, the endocrine signal thyroid hormone (TH) regulates differential expression of the orthologous zebrafish *lws1/lws2* array, and of the tandemly quadruplicated *rh2-1/rh2-2/rh2-3/rh2-4* array. TH treatment caused dramatic, dose-dependent increases in abundance of *lws1*, the proximal member of the *lws* array, and reduced *lws2*. Fluorescent *lws* reporters permitted direct visualization of individual cones switching expression from *lws2* to *lws1*. Athyroidism increased *lws2* and reduced *lws1*, except within a small ventral domain of *lws1* that was likely sustained by retinoic acid signaling. Changes in *lws* abundance and distribution in athyroid zebrafish were rescued by TH, demonstrating plasticity of cone phenotype in response to this signal. TH manipulations also regulated the *rh2* array, with athyroidism reducing abundance of distal members. Interestingly, the opsins encoded by the proximal *lws* gene and distal *rh2* genes are sensitive to longer wavelengths than other members of their respective arrays; therefore, endogenous TH acts upon each opsin array to shift overall spectral sensitivity toward longer wavelengths, underlying coordinated changes in visual system function during development and growth.

zebrafish | cone | thyroid hormone | retina | opsin

Cone photoreceptors of the vertebrate retina mediate daylight vision and are critical for high-acuity vision and color discrimination. Cone types are determined by the opsin protein expressed. Vertebrate cone opsins are classified into 4 phylogenetic types: SWS1 (short wavelength-sensitive type 1, UV-blue), SWS2 (short wavelength-sensitive type 2, blue), RH2 (medium wavelength-sensitive, green), and M/LWS (medium to long wavelength-sensitive, red) (1). Humans have 3 cone types: *LWS* (red), *MWS* (green), and *SWS1* (blue) (2). The *LWS* and *MWS* opsin genes are arranged in a tail-to-head manner on the X chromosome, and are expressed in separate cone populations (3). The choice of *LWS* or *MWS* expression is thought to be a stochastic event. In the current model, an upstream locus control region (LCR) preferentially associates with either the *LWS* or *MWS* promoter (4). This association then becomes permanent, resulting in mutually exclusive expression of only 1 of the opsin genes from the array (4). However, this stochastic model does not explain the relative distribution of *LWS* vs. *MWS* cones as a function of retinal eccentricity, with *LWS*:*MWS* ratios higher in peripheral than in central retina (5). This gradient suggests the potential for additional, transregulatory mechanisms.

Fish are the only other vertebrate taxonomic group besides primates known to contain tandemly replicated opsin genes (6). In zebrafish, the *lws1* gene (orthologous to human *LWS*) has undergone a tandem replication (independent of the *LWS*/*MWS* replication event in humans) resulting in a second member (*lws2*)

encoding an opsin with a shorter wavelength-shifted sensitivity (7). The zebrafish *lws* locus contains an upstream regulatory region, termed the *LWS* activating region (LAR) that is required for proper expression of either member of the array (8). The adult zebrafish displays an *lws1/lws2* gradient similar to the *LWS*/*MWS* gradient in humans (5), with an *lws1:lws2* ratio lower in the central retina compared with the periphery (9). During zebrafish retinal development, *lws1* expression is absent in the early larval retina; onset of its expression occurs in ventral retina at approximately 6 d postfertilization (6 dpf) (9). The expression domain of *lws1* then expands into nasal/dorsal retina in juveniles and remains in the periphery throughout the remainder of fish growth (9). These dynamic spatiotemporal expression patterns, and changes in *lws1/lws2* ratio seen during development, further indicate that regulation of these tandemly replicated opsin genes goes beyond a stochastic mechanism. Indeed, we recently demonstrated that the paracrine signal retinoic acid (RA) is involved in differentially regulating *lws1* vs. *lws2* (10). Exogenous RA treatment of embryos during photoreceptor differentiation resulted in increased *lws1* and a decrease in *lws2*. Conversely, *lws1* was decreased when RA signaling was reduced. However, *lws2* expression was either decreased or unaffected by reduced RA signaling, suggesting other factors are likely involved in the endogenous regulation of *lws2*. This (10) was the first reported evidence of a transacting mechanism involved in differentially regulating tandemly replicated opsin genes, providing evidence of regulation beyond a stochastic mechanism.

In addition to the tandemly duplicated *lws* opsins, the *rh2* cone opsin array in zebrafish has been tandemly quadruplicated (7).

Significance

Primate and fish genomes contain tandemly replicated cone opsin genes. The human long wavelength-sensitive/medium wavelength-sensitive (*LWS*/*MWS*) tandem array underlies trichromatic color vision; mutations in this array cause altered color vision and retinal degenerations. Differential expression of human *LWS* vs. *MWS* is considered a stochastic event, whereby upstream enhancers associate with the promoter of the proximal or distal gene. We demonstrate that the endocrine signal thyroid hormone (TH) is a potent endogenous regulator of the orthologous zebrafish *lws1/lws2* array, and of the tandemly quadruplicated *rh2-1/rh2-2/rh2-3/rh2-4* array. TH promotes shifts in spectral sensitivity to longer wavelengths by changing expression of opsins in each array, indicating TH-coordinated control of visual function during organismal growth.

Author contributions: R.D.M., S.K., D.M.M., and D.L.S. designed research; R.D.M., R.A.F., C.G., and A.A.F. performed research; S.K. contributed new reagents/analytic tools; R.D.M., S.K., D.M.M., and D.L.S. analyzed data; and R.D.M., S.K., D.M.M., and D.L.S. wrote the paper.

The authors declare no conflict of interest.

This article is an PNAS Direct Submission. R.J. is a guest editor invited by the Editorial Board.

This open access article is distributed under Creative Commons Attribution-NonCommercial-NoDerivatives License 4.0 (CC BY-NC-ND).

¹To whom correspondence may be addressed. Email: dstenkam@uidaho.edu.

This article contains supporting information online at www.pnas.org/lookup/suppl/doi:10.1073/pnas.1904783116/-DCSupplemental.

Published online August 5, 2019.

The *rh2* array has an upstream LCR required for the expression of any of the 4 opsin genes (11). In contrast with the *lws* array, the *rh2* gene encoding the longest wavelength-sensitive opsin (*rh2-4*) is most distally positioned, while that encoding the shortest wavelength-sensitive opsin (*rh2-1*) is most proximally positioned on the array. The *rh2-1* expression domain, like the *lws2* domain, is widespread throughout the larval retina, then recedes in the periphery and is isolated to central retina in juveniles and adults (9). *rh2-2* expression is also widespread throughout the larval retina, recedes from central retina in juveniles, but is restored in the central retina of adults (9). Expression of both *rh2-3* and *rh2-4* remains low and restricted to peripheral regions throughout life. In summary, expression of the shorter wavelength-sensitive members of both the *lws* and *rh2* arrays occurs before the longer wavelength-sensitive members, and in adult retina the shorter wavelength-sensitive members are expressed in the central/dorsal retina, while longer wavelength-sensitive members are expressed in ventral/peripheral areas (9). The mechanisms governing these dynamic changes in expression patterns throughout development and growth have not been fully elucidated, but the establishment of the adult patterns is known to involve *cis*-elements in upstream and intergenic regions and the relative proximal-to-distal position of each member of the array (12).

The endocrine signal thyroid hormone (TH) plays a pivotal role in the development of the retina, specifically in cone differentiation (13–18). TH is synthesized in the thyroid as tetraiodothyronine (thyroxine; T₄). T₄ enters the circulatory system where in the periphery it is converted into tri-iodothyronine (T₃) by the cellular enzyme deiodinase 2 (Dio2) (19). T₃ binds to nuclear TH receptors to regulate gene expression. In addition to TH homodimers, TH receptors can heterodimerize with retinoid X receptors (RXRs) to influence gene expression (20). Considering our previous work (10), accompanied by the known involvement of TH in regulating opsin expression in other organisms (21–23), we hypothesized that TH may also be involved in the differential regulation of the tandemly duplicated *lws* opsin genes in zebrafish. We performed gain-of-function (GOF) studies involving a TH (T₃) treatment regimen 2 to 4 dpf, a time of *lws2* expression but prior to the normal onset of expression of *lws1* (9). Utilizing qRT-PCR, in situ hybridization, and transgenic zebrafish reporting *lws1* and *lws2* expression (8), we identified TH as a potent regulator of differential expression of tandemly replicated opsins in zebrafish, including both the *lws* and *rh2* opsin arrays. Loss-of-function (LOF) and T₃ localization studies provided further evidence of TH's endogenous role in this regulatory mechanism. Furthermore, we demonstrated that expression of tandemly replicated opsin genes remains plastic and can be influenced by TH exposure in both normal and athyroid juvenile zebrafish.

Results

TH Treatment Alters Relative Expression Levels and Patterns of *lws* Opsin Transcripts. To test our hypothesis that TH signaling regulates the differential expression of tandemly replicated opsin genes, we augmented levels of TH in wild-type zebrafish embryos/larvae by immersion in 4, 20, or 100 nM T₃ from 2 to 4 dpf and determined the effects on *lws1* vs. *lws2* expression in comparison to a control (0.1% DMSO) treatment. qPCR revealed that T₃ treatment resulted in a strong dose-dependent increase in *lws1* transcript abundance (Fig. 1A), with up to a 1,000-fold increase compared to control at the highest T₃ concentration (Fig. 1A). Abundance of *lws2* did not change due to 4 nM or 20 nM T₃ treatment but decreased as much as 30-fold with the highest concentration (Fig. 1B). T₃ was much more effective than retinoids, since retinoids increased *lws1* 3-fold and decreased *lws2* 2- to 5-fold (10). We then employed in situ hybridization using transcript-specific probes for both members of the *lws* array. *lws1* was not detected in cryosectioned, control retinas at 4 dpf, consistent with previous reports indicating that the normal onset of expression of *lws1* is ~6 dpf (9). In T₃-treated larvae, expression of *lws1* in the outer nuclear layer (ONL, containing photoreceptors) was detected at 4 dpf, and included dramatic expansion of the

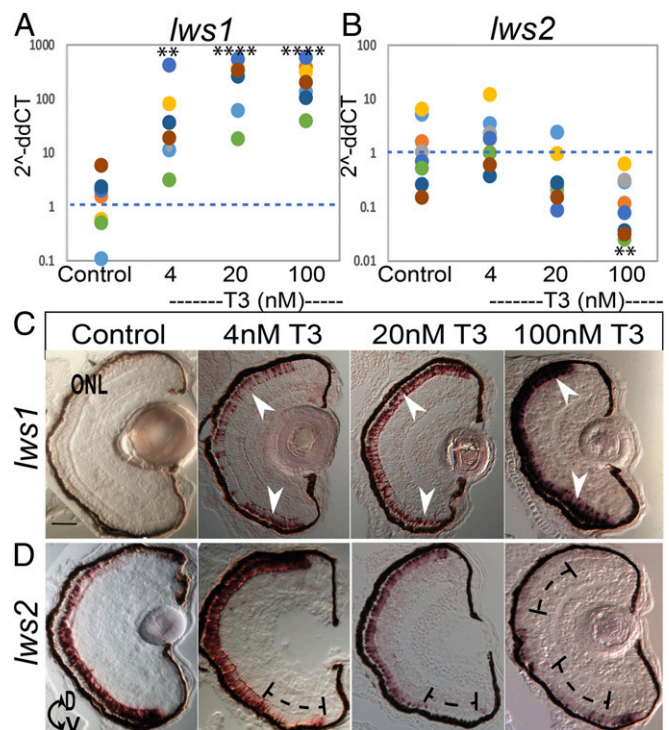


Fig. 1. qPCR and in situ hybridization for *lws* transcript abundance reveals robust differential regulation after TH (T₃) treatment from 2 to 4 dpf. (A and B) Scatter plots indicate fold-change (2^{-ddCT}) abundance of the indicated transcripts. Colors of dots correspond to separate experiments. Each dot represents 1 biological sample (pooled RNA from ~5 larvae). For each condition $n = 8$ (A). *lws1* abundance in DMSO control, increased by 4 nM T₃ $P = 0.001502$, increased by 20 nM T₃ $P = 0.000003$, increased by 100 nM T₃ $P = 0.000002$. (B) *lws2* abundance in control was unchanged by both 4 nM T₃ and 20 nM T₃ $P = 0.288195$ and $P = 0.073120$ but decreased by 100 nM T₃ $P = 0.004823$. P values were calculated by comparing the ddCT values for treated vs. control from each experiment using the Kruskal–Wallis test and the Conover post hoc test further adjusted by the Benjamini–Hochberg false-discovery rate method. Statistical notation: $**P < 0.01$, $****P < 0.0001$. (C and D) In situ hybridization of cryosectioned eyes using gene-specific probes for *lws1* (C) and *lws2* (D) from larvae treated 2 to 4 dpf with DMSO (control) or T₃. Arrows in C indicate induced and expanded expression domain of *lws1* due to T₃ treatment; brackets in D indicate regions showing reduced expression of *lws2* due to T₃ treatment. D, dorsal; V, ventral. (Scale bar in C and D), 50 μ m.)

expression domain (Fig. 1C). Expression of *lws1* appeared most concentrated in the ventral retina and expanded dorsally with increasing T₃. *lws2* expression in controls was widespread throughout the retina, consistent with previous reports (9), but diminished with increasing amounts of T₃ (Fig. 1D). Ventral retina became progressively *lws2*-depleted by 4 nM and by 20 nM T₃, while a more complex pattern of remnant *lws2* expression resulted from 100 nM T₃ (Fig. 1D). These findings demonstrate a robust effect of exogenous TH on relative levels of *lws1* vs. *lws2* transcript, together with substantial changes of their expression domains.

Global Patterns of *lws1* and *lws2* in the Developing Retina Are Altered Due to TH Treatment. To better visualize the spatial distribution of *lws1/lws2* expression in the developing retina, as well as any cones coexpressing both opsins, we utilized a transgenic line *Tg(LWS1/GFP-LWS2/RFP-PAC(H)) #430* (8), which we refer to as *lws:PAC(H)*. This line reports *lws1* expression with GFP and *lws2* with RFP, and faithfully reports the native expression patterns of the 2 opsins (8), albeit with a slight delay in *lws2* (RFP) expression in comparison with native transcript (10). *lws:PAC(H)* embryos were treated with T₃ or DMSO (control) from 2 to 4 dpf. RFP⁺ (*lws2*) cones were detected in cryosections

from control embryos throughout most of the retina (Fig. 2A). GFP⁺ (*lws1*⁺) cones were not detected in controls at 4 dpf (Fig. 2A). In contrast, in T3-treated embryos, GFP⁺ cones were detected in ventral retina (Fig. 2B), which matches the location of later, endogenous onset of *lws1* expression (9). With increasing concentrations of T3, the distribution of GFP⁺ cells expanded into central and dorsal retina (Fig. 2C and D).

When we examined whole retinas, RFP⁺ (*lws2*⁺) cones were detected in control embryos throughout most of the retina, but little to no RFP was present in the dorsal/temporal region. Again, GFP⁺ (*lws1*⁺) cones were not detected in control embryos at 4 dpf (Fig. 2E). Corroborating our results from cryosections, in 4 nM T3-treated embryos, GFP⁺ cones were detected in the ventral retina (Fig. 2F). With increasing concentrations of T3, the distribution of GFP⁺ cones expanded nasally and dorsally (Fig. 2G and H). Areas displaying increased numbers of GFP⁺ cones included a ventral patch and a dorsal/nasal area largely isolated to the periphery. T3 caused dose-dependent increases in the number of GFP⁺ cones (Fig. 2I), and in the number of colabeled cones (Fig. 2K). These colabeled cones simultaneously expressed both reporters, suggesting that these cones were switching expression from *lws2* to *lws1*. The numbers of RFP⁺ (*lws2*⁺) cones were significantly reduced with the highest concentration of T3 (Fig. 2J). These results, together with evidence from qPCR and in situ hybridization, suggest that the dramatic increase in *lws1* is at the expense of *lws2* expression in individual LWS cones. Alternatively, or in addition, coexpressing cells could be explained by transcription of *lws1* from 1 allele while *lws2* is transcribed from the other.

Exogenous TH Triggers Opsin Switching in Individual Cones. We used 2 complementary strategies to determine whether individual LWS cones engage in “opsin switching” in response to T3: live confocal imaging and 2D pattern analysis of the LWS cone mosaic (24), both using the *lws:PAC(H)* transgenic zebrafish. To directly observe LWS cones switching opsin expression in real time, we treated *lws:PAC(H)* larvae with 100 nM T3, and imaged ventral retina for 9 h at 40× magnification starting 8 h after the T3 treatment began. Time-lapse video revealed that some RFP⁺ cones began to express GFP, showing domains of coexpression that then expanded within each cone, followed by a switch to primarily GFP expression, with some remaining coexpression (Fig. 3 and Movie S1). These results strongly support a switch from *lws2* to *lws1* in individual LWS cones in response to the T3 treatment.

The rationale for 2D pattern analysis is that, if an *lws2*-to-*lws1* switch (RFP to GFP) takes place within individual cones, versus recruiting other cone types to express *lws1* (GFP), then T3 treatment should result in no disruption of the spatial arrangement of LWS cones labeled by either or both reporters (10). Average nearest-neighbor distances (NNDs) (*SI Appendix, SI Methods*) were similar for RFP⁺ cones in untreated larvae in comparison with the entire population of labeled cones (GFP⁺ and RFP⁺) in treated larvae, suggesting that the GFP⁺ cones did not disrupt the pattern of LWS cones (*SI Appendix, Fig. S1*). However, the combined GFP⁺ and RFP⁺ average NND was greater than that of the GFP⁺ cones, consistent with the GFP⁺ cones comprising a fraction of a total LWS cone population (*SI Appendix, Fig. S1E*). Calculating the regularity index (RI: mean NND/SD, adjusted for object density) (24, 25) as a measure of pattern regularity (*SI Appendix, Fig. S1F*), and comparing each selected region with 1,000 random simulations having the same number of objects (*SI Appendix, Fig. S1G*) revealed no differences among groups for both the RI, and the $RI_{\text{sample}}/RI_{\text{random}}$, suggesting that the presence of GFP⁺ cones in T3-treated samples did not disrupt the regular cone mosaic (*SI Appendix, Fig. S1 F and G*).

A Time-Course Treatment with TH Reveals Kinetics of Changes in *lws* Expression. *Lws* expression was analyzed in larvae after different durations of 100 nM T3 treatment (*SI Appendix, SI Methods*). After 12 h of treatment (ht) beginning at 2 dpf, abundance of

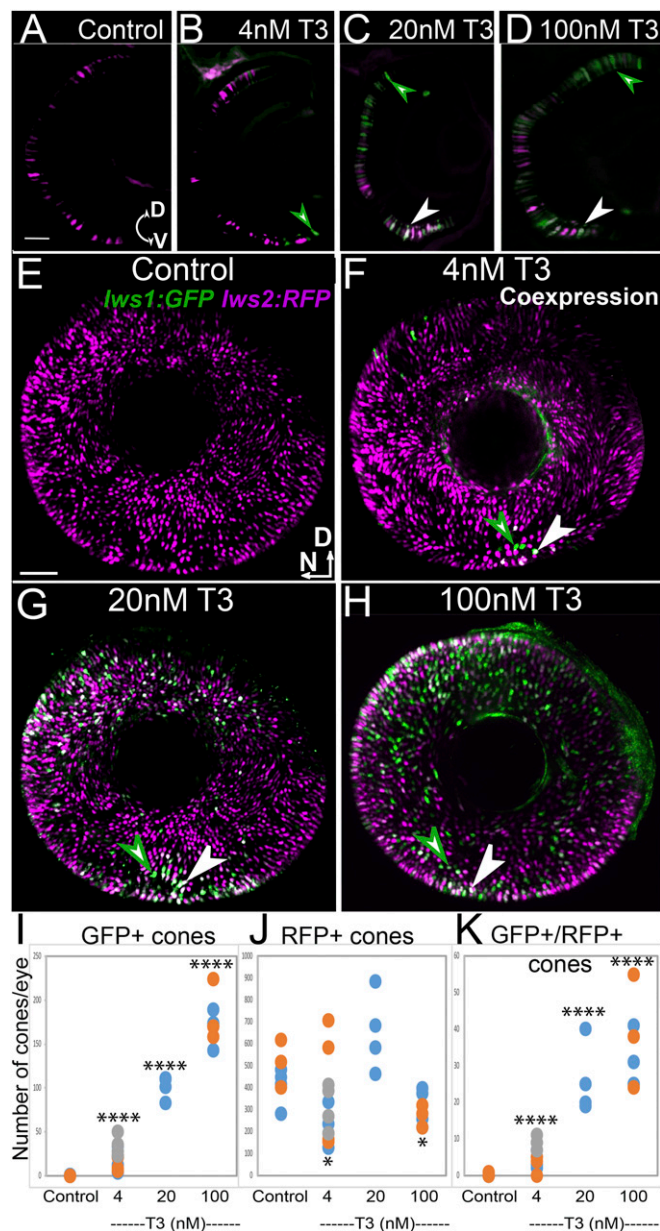


Fig. 2. *Lws* reporter transgenic indicates a switch from *lws2* to *lws1* in response to TH (T3). (A–D) Cryosections from 4 dpf *lws:PAC(H)* eyes treated with DMSO (control; A), 4 nM T3 (B), 20 nM T3 (C), 100 nM T3 (D). (E–H) Whole-mounted *lws:PAC(H)* eyes visualized by confocal microscopy of DMSO (control) (E), 4 nM T3 (F), 20 nM T3 (G), 100 nM T3 (H). Green arrowheads indicate GFP⁺ cones, white arrowheads indicate colabeled cones. RFP is pseudocolored magenta. D, dorsal; N, nasal; V, ventral. (Scale bars in A [applies to A–D] and E [applies to E–H], 50 μm .) (I–K) GFP⁺ cone numbers, 4 nM T3 $P = 1.28\text{e-}07$, 20 nM T3 $P = 2.47\text{e-}10$, 100 nM T3 $P = 4.46\text{e-}14$ (I). RFP⁺ cones 4 nM T3 $P = 0.022$, 20 nM T3 $P = 0.25$, 100 nM T3 $P = 0.03$ (J) and (K) GFP⁺/RFP⁺ cone numbers, 4 nM T3 $P = 2.3\text{e-}05$, 20 nM T3 $P = 9.8\text{e-}09$, 100 nM T3 $P = 4.0\text{e-}11$ from 3 z-projected images from whole mounts of each condition show a dose-dependent increase in GFP-expressing (*lws1*⁺) cones. Colors of dots correspond to separate experiments. Each dot represents a biological replicate (an individual larva). P values were calculated by comparing the number of GFP⁺ or GFP⁺/RFP⁺ cones for treated vs. control from each experiment using the Kruskal–Wallis test and the Conover post hoc test further adjusted by the Benjamini–Hochberg false-discovery rate method. Statistical notation: * $P < 0.05$, **** $P < 0.0001$.

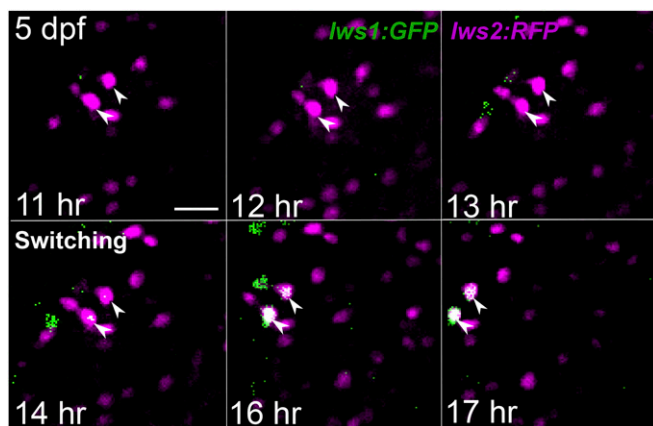


Fig. 3. Live imaging of 5 dpf *lws:PAC(H)* *lws* reporter transgenic confirms a switch from *lws2* to *lws1* in individual cones in response to TH (T3). Imaging was conducted for 9 h starting 8 h after treatment with 100 nM T3 began. Time stamps indicate hours from start of imaging. Arrowheads show 2 RFP+ (*lws2*⁺) cones switching to express GFP (*lws1*) over the time of imaging. Cells move to the left of the region of interest due to growth of the larva. (Scale bar, 10 μ m.)

lws1 and *lws2* transcripts were unchanged (SI Appendix, Fig. S2A and B). By 24 ht, the magnitude of *lws1* increase was 85-fold higher compared with controls (SI Appendix, Fig. S2A), while in contrast *lws2* levels were unchanged (SI Appendix, Fig. S2B), suggesting complex temporal kinetics. The changes in transcript abundance were most pronounced when embryos were treated from 2 to 4 dpf (SI Appendix, Fig. S2A and B; see also Fig. 1A).

In similar time-course experiments using the *lws:PAC(H)* transgenics, a few GFP⁺ (*lws1*⁺) cones were detected after 12 ht (treatment beginning at 2 dpf) in the ventral retina (SI Appendix, Fig. S2C), and at 24 ht GFP⁺ cones increased in number and retinas displayed dorsal expansion of regions containing GFP⁺ cones (SI Appendix, Fig. S2D). GFP⁺ cones were not detected at 4 dpf (Fig. 2A). At 24 ht RFP⁺ (*lws2*⁺) cones were initially detected along with colabeled cones in the ventral retina of T3 treated embryos (SI Appendix, Fig. S2D). By 48 ht the RFP⁺ cones were detected throughout the retina, as well as GFP⁺ and colabeled cones in the ventral retina and dorsal/nasal area in T3-treated embryos (SI Appendix, Fig. S2E).

T3 Accumulates in LWS Cones upon Exogenous Treatment. We wished to determine whether LWS cones accumulate T3 in embryos/larvae exposed to exogenous T3, consistent with a potentially cell-autonomous mechanism. LWS cones express *thyroid hormone receptor* $\beta 2$ (*tr\beta 2*) (26). We utilized a transgenic line that reports *tr\beta 2* with tdTomato to label all LWS cones (26), and crossed it to a “ligand trap” transgenic that reports the intracellular presence of T3 with GFP (27, 28). Embryos from this cross were treated with 100 nM T3 starting at 2 dpf. In nontreated embryos, the ligand trap did not detect endogenous levels of T3 (27). With 100 nM T3, GFP⁺ cells reporting T3 accumulation were observed in multiple retinal layers, including many in the ONL, at both 3 and 4 dpf (Fig. 4). Many, but not all, of the GFP⁺ cells (T3-accumulating) of the ONL coexpressed the *tr\beta 2* reporter, and numerous, but not all, of the tdTomato⁺ (LWS cones) coexpressed GFP (Fig. 4, Insets). The fraction of LWS cones accumulating T3 appeared consistent with the fraction of LWS cones that switch from *lws2* to *lws1* expression (Fig. 2H), leaving open the potential for a cell-autonomous mechanism. The spatial distribution of GFP⁺ (T3 accumulating) cones did not appear to change from 3 to 4 dpf (Fig. 4).

Ablation of the Thyroid Gland Suppresses the Onset of Endogenous *lws1* Expression. To evaluate endogenous roles for TH in *lws* regulation, we utilized a transgenic line *Tg(tg:nVenus-2a-nfnB)*^{wp.rn8} in which the thyroid gland is ablated upon metronidazole treatment (29). To minimize the levels of circulating TH and to

attenuate its synthesis, we experimentally ablated the thyroid in *Tg(tg:nVenus-2a-nfnB)*^{wp.rn8} fish at 2 dpf, when the zebrafish thyroid becomes active (30). Athyroidism was confirmed by the absence of the Venus YFP reporter-expressing thyroglobulin cells following metronidazole treatment (Fig. 5A and B). When measured by qPCR, *lws1* transcript was detected in control larvae at 6 dpf. *Lws1* was suppressed in athyroid larvae, consistent with an endogenous role for TH in controlling *lws1* expression (Fig. 5C). However, *lws2* levels were not different in athyroid larvae compared to controls (Fig. 5D) at this time point.

Crossing *lws:PAC(H)* with *Tg(tg:nVenus-2a-nfnB)*^{wp.rn8} allowed visualization of *lws* expression via fluorescent reporters in 6-dpf larvae with an active thyroid compared to athyroid larvae. In controls, a small number of GFP⁺ (*lws1*⁺) cones were detected in the ventral retina at 6 dpf (Fig. 5E). In contrast, in athyroid larvae, GFP⁺ cones were not detected (Fig. 5F). Collectively, these results support an endogenous role for embryonically derived TH in inducing *lws1* expression in LWS cones at the time of normal onset of *lws1* expression.

Lws Differential Expression Remains Plastic to the Effects of TH Signaling through Juvenile Growth. We next investigated longer lasting effects of athyroidism on *lws* opsin expression and the plasticity of *lws* expression in response to exogenous TH in growing juvenile zebrafish (Fig. 6A). From 26 to 31 dpf, the *lws1* expression domain expands to cover much of ventral and nasal retina (9). Exogenous T4 (GOF) over this time did not alter levels of *lws1* transcript, compared to controls (Fig. 6B); however, *lws2* was reduced by 30-fold (Fig. 6C), indicating that in juvenile zebrafish, LWS cones are plastic to the effects of TH

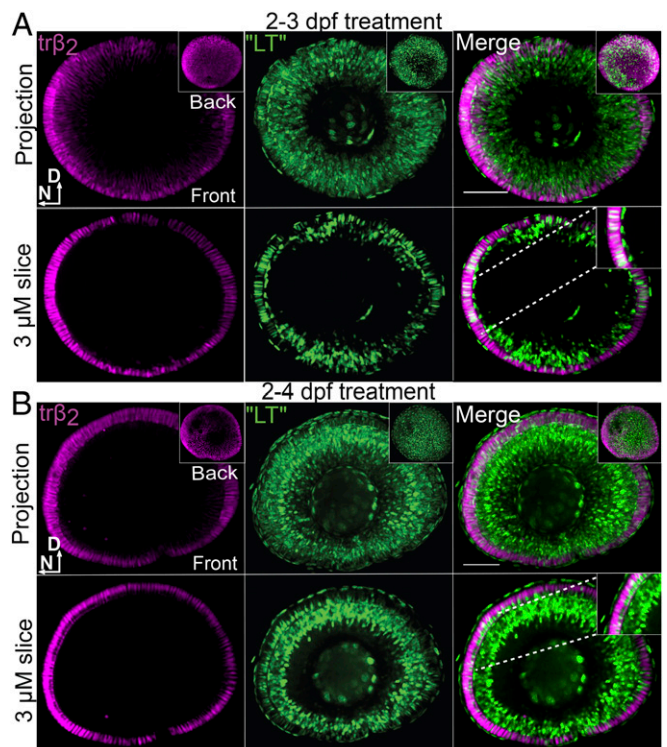


Fig. 4. TH “ligand trap” reporter transgenic and *tr\beta 2* reporter transgenic indicate accumulation of TH (T3) in *lws*⁺ (*TR\beta 2*⁺) cones after T3 treatment. All panels include visualization of T3 accumulation (ligand trap, GFP⁺), *tr\beta 2*⁺ cones (tdTomato⁺), and merge (colabeled cells are white) of whole-mounted eyes visualized by confocal microscopy, from larvae treated with 100 nM T3 from 2 to 3 dpf (A) or 2 to 4 dpf (B). D, dorsal; N, nasal. Insets in Upper rows of A and B show views of the back of the eye; Insets in Lower rows of A and B show higher magnification of a single 3- μ m z-slice to visualize coexpressing cones. (Scale bars, 50 μ m.)

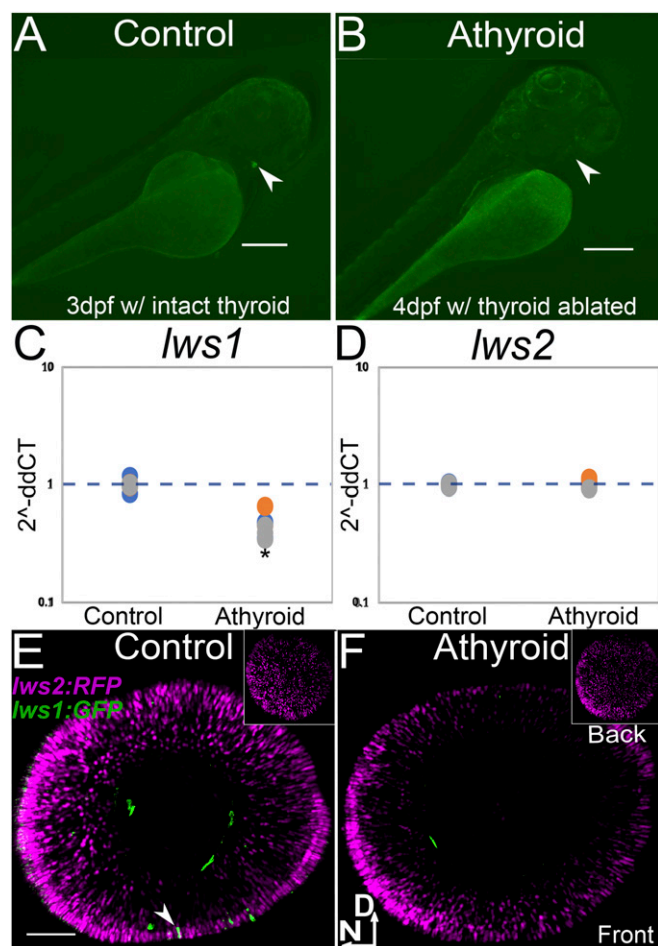


Fig. 5. TH LOF by thyroid ablation suppresses *lws1* expression at time of native onset of expression. (A and B) Transgenic [*Tg(tg:nVenus-2a-nfnB)*]^{wp.rts} that allows for thyroid ablation mediated by metronidazole treatment and nitroreductase expressing thyroglobulin cells) with intact thyroid, indicated by Venus (YFP) expression in embryo (A, arrowhead) and thyroid ablation, indicated by absence of Venus (YFP) (arrowhead shows normal location of thyroid gland) after 24-h treatment with metronidazole (B). (Scale bars in A and B, 250 μm .) (C and D) qPCR abundance of *lws1* (C) and *lws2* (D) transcripts (fold-change, $2^{-\Delta\Delta\text{CT}}$) in 6 dpf DMSO (control) and athyroid larvae. In comparison to control ($n = 3$) samples, *lws1* is reduced in athyroid larvae ($n = 3$) $P = 0.04$ (C), and *lws2* is not changed in athyroid larvae ($n = 3$) $P = 0.32$ (D). P values were calculated by comparing the ddCT values for the thyroid-ablated groups vs. controls from each experiment using a Wilcoxon Mann-Whitney U test. Statistical notation: * $P < 0.05$. (E and F) *lws:PAC(H)* *lws* reporter transgenic, whole-mounted eyes visualized by confocal microscopy of 6 dpf DMSO (control) (E) and athyroid larvae (F). Insets show views of the back of the eye; arrowhead in E indicates an *lws1* (GFP⁺)-expressing cone; D, dorsal; N, nasal. (Scale bar in E [applies to E and F], 50 μm .)

signaling. Following thyroid ablation of *Tg(tg:nVenus-2a-nfnB)*^{wp.rts} embryos at 2 dpf, half of the group was immersed in 386 nM T4 from 26 to 31 dpf (as in ref. 31) (Fig. 6A). In athyroid juveniles (LOF), *lws1* levels were reduced by 15.6-fold and *lws2* was increased by 1.87-fold compared to controls (Fig. 6B and C), supporting roles for endogenous thyroid signaling in both promoting *lws1* expression and reducing *lws2* expression. In athyroid juveniles rescued with T4 (Rescue), abundance of *lws1* transcript was increased by 22-fold, compared with athyroid juveniles (Fig. 6B), and *lws2* was reduced 90-fold (Fig. 6C), indicating that T4 rescued the effects of athyroidism. Collectively these results demonstrate that *lws1* vs. *lws2* expression can be differentially regulated post-embryonically, and that LWS cones remain plastic to the effects of TH, even in the case of prolonged athyroidism.

Performing the same experiments in the *lws:PAC(H)* transgenics crossed with *Tg(tg:nVenus-2a-nfnB)*^{wp.rts} provided valuable insight into retinal topographic changes in expression of *lws1* vs. *lws2*. In control juveniles, GFP⁺ (*lws1*⁺) cones were detected in ventral, nasal, and dorsal retina, and RFP⁺ (*lws2*⁺) cones were predominantly observed in central retina, consistent with known patterns of expression of endogenous transcript at this age (9, 10) (Fig. 6D). In T4-treated juveniles (GOF), GFP⁺ cones were detected throughout the peripheral retina, with numerous GFP⁺ cones in central retina also expressing RFP (Fig. 6E and I). In athyroid juveniles (LOF), GFP⁺ cones were restricted to a ventral sector of the retina, with no nasal or dorsal expansion (Fig. 6F). We previously reported a ventral region of juvenile retina in which RA signaling matches a region of *lws1* expression (10). Whole-mounted retinas derived from juvenile (age-matched) *RARE:YFP* transgenic fish in which YFP expression is driven by 4 consecutive retinoic acid response elements (RAREs) (32), more precisely revealed this RA signaling domain (Fig. 6H). This domain spatially correlates to the restricted domain of *lws1* expression in the athyroid juvenile retinas, suggesting that in the absence of TH, RA signaling in ventral retina is sufficient to promote *lws1* at the expense of *lws2*. In athyroid juveniles rescued with T4 (Rescue), GFP⁺ cones were detected throughout the peripheral retina, and numerous GFP⁺ cones in central retina also expressed RFP (Fig. 6G).

Collectively these results suggest that *lws1* expression in the ventral retina is sustained by RA signaling in athyroid juveniles, but the nasal/dorsal expansion of the *lws1* expression domain requires TH signaling, and can be rescued by T4. These results also provided further evidence that *lws1* vs. *lws2* expression remains plastic and is amenable to TH signaling at least into the juvenile stage of zebrafish growth. We previously reported the presence of predicted consensus RAREs on the *lws* locus (10). We reanalyzed the zebrafish *lws* locus for putative response elements for both TH (TRE) and RA/RXR (RARE/RXRE) (*SI Appendix, SI Methods*), and identified several of these elements upstream from the coding sequence of both genes (*SI Appendix, Fig. S3A*), suggesting the possibility of direct regulatory mechanisms involving both RA and TH.

Differential Expression of *rh2-1*, *rh2-2*, and *rh2-3* Opsins upon T3 Treatment. The tandemly quadruplicated *rh2* MWS (*opn1mw*) opsin gene locus contains *rh2-1*, *rh2-2*, *rh2-3*, and *rh2-4* genes. To test the hypothesis that TH also regulates differential expression from this array, we performed dose-response T3 studies in larvae, and determined the effects on all 4 *rh2* transcripts in comparison to a control (0.1% DMSO) treatment. During normal development, at 3 dpf, *rh2-1* is expressed in ventral, dorsal, and nasal retina, while *rh2-2* is not detected (9). qPCR revealed that the levels of these 2 *rh2* transcripts were affected in T3-treated (from 2 to 4 dpf) larvae. Abundance of *rh2-1* was not changed due to 4 nM T3 treatment but was decreased 2-fold by the higher doses (Fig. 7A). Levels of *rh2-2* were increased by 8.9-fold, 6.7-fold, and 7-fold by 4, 20, and 100 nM T3, respectively (Fig. 7B). Interestingly, in nearly all control (0.1% DMSO) samples, *rh2-3* and *rh2-4* transcripts were not detectable, or unreliably detectable (*SI Appendix, Table S1*). However, in larvae treated with 100 nM T3, *rh2-3* transcript was detectable in all samples, while *rh2-4* was detectable only in 3 of the 6 biological replicates (*SI Appendix, Table S1*). These results collectively suggest that components of the zebrafish *rh2* opsin gene array can be regulated by exogenous T3 in larval zebrafish.

We then employed in situ hybridization using gene-specific probes for all 4 members of the *rh2* locus. *rh2-1* expression in controls was widespread throughout the retina, consistent with previous reports (9), but was diminished with increasing amounts of T3 (Fig. 7C). Ventral and dorsal retina was depleted of *rh2-1* by 4 nM T3 and little to no *rh2-1* transcript was detected with 20 and 100 nM T3, except for a small patch remaining in the central retina (Fig. 7C). *rh2-2* was not detected in controls, but was expressed in T3-treated larvae, with larger expression domains

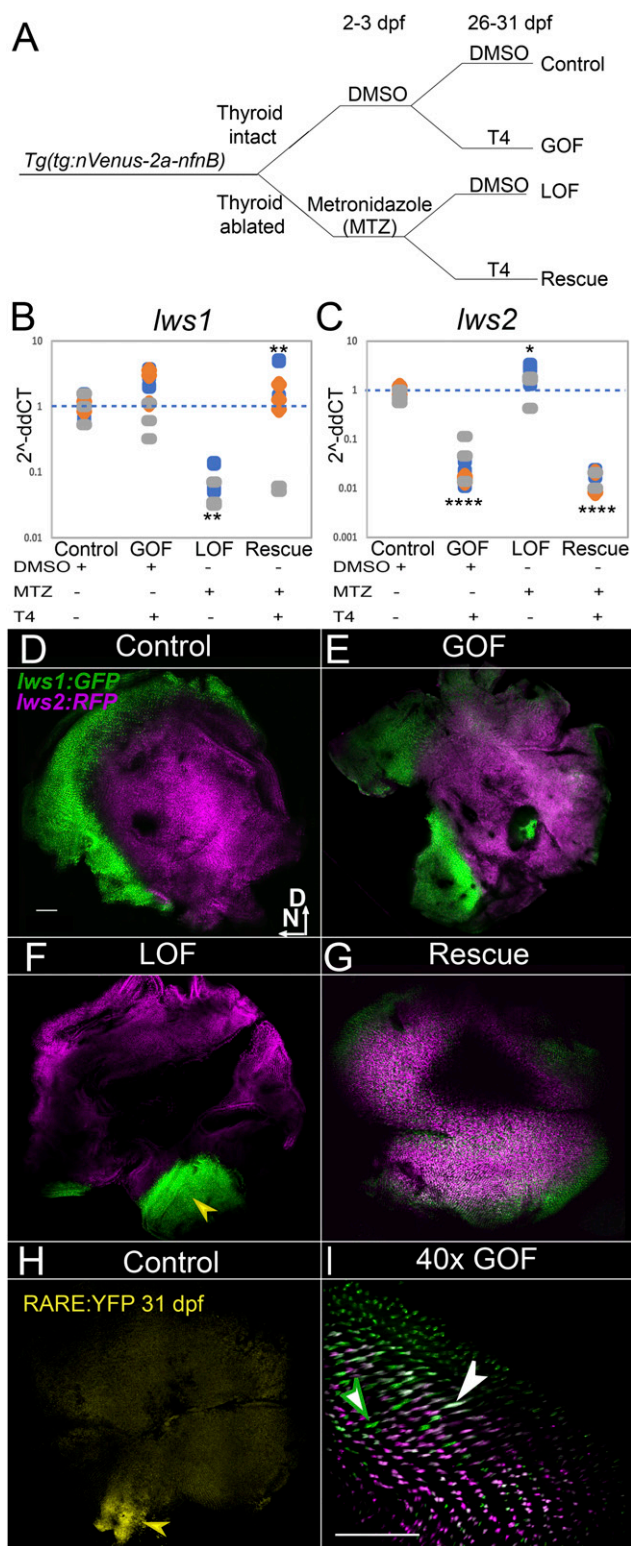


Fig. 6. Plasticity of *lws* differential expression by TH (T4) in normal and athyroid juveniles. (A) Schematic of experimental workflow including thyroid ablation at 2 dpf followed by T4 treatment starting at 26 dpf for 5 d, of half the athyroid group and half of the controls. (B and C) qPCR of *lws1* (A) and *lws2* (B) transcript abundance. Scatter plots indicate fold-change abundance ($2^{-\Delta\text{ddCT}}$) of the indicated transcripts. Colors of dots correspond to separate experiments. Each dot represents a biological replicate (2 retinas from an individual fish). *lws1* abundance (B) in DMSO (control) ($n = 9$), is unchanged by T4 GOF ($n = 9$) $P = 0.21$ compared to control, decreased in athyroid (LOF) ($n = 6$) $P = 0.006$ compared to control, and increased in Rescue

resulting from higher doses (Fig. 7D). Control sections showed no in situ hybridization signal for either *rh2-3* or *rh2-4* (SI Appendix, Fig. S4), indicating that transcript levels were below detectable range. We were also unable to detect either of these transcripts in sections of T3-treated larvae (SI Appendix, Fig. S4). It is possible that the levels of *rh2-3* detectable by qPCR (SI Appendix, Table S1) cannot be visualized by in situ hybridization, or that the sections used for this analysis did not contain the likely rare *rh2-3*⁺ cone. These outcomes for TH regulation of the *rh2* array are particularly striking because T3 promotes the most proximal gene of the *lws* array (*lws1*), but more distal genes of the *rh2* array (*rh2-2*, *rh2-3*) in larvae, suggesting that, while the general function of TH is conserved, the precise molecular mechanism may be distinct.

Rh2 Differential Expression Remains Plastic to the Effects of TH Signaling through Juvenile Growth. We next investigated longer lasting effects of athyroidism on *rh2* opsin expression and the plasticity of *rh2* expression in juvenile zebrafish, using the experimental design shown in Fig. 6A. In juveniles treated with T4 (GOF), *rh2-1* transcript levels were reduced by 93-fold (Fig. 8A), and abundance of *rh2-3* was increased by 1.8-fold (Fig. 8C). Levels of *rh2-2* and *rh2-4* were unchanged in comparison with controls (Fig. 8B and D). In athyroid juveniles (LOF), *rh2-1* levels were not different (Fig. 8A), while levels of *rh2-2*, *rh2-3*, and *rh2-4* transcripts were reduced by 5.3-fold, 9.8-fold, and 2.2-fold, respectively, compared to controls (Fig. 8B–D). In athyroid juveniles treated with T4 (Rescue), *rh2-1* was decreased 477-fold, *rh2-2* was not changed, while abundance of *rh2-3* and *rh2-4* transcripts was increased 11-fold and 7-fold, respectively (rescued), compared to athyroid juveniles (Fig. 8B–D). To summarize, TH GOF drastically decreased *rh2-1* but not *rh2-2* and *rh2-4*, while *rh2-3* was increased. Surprisingly, TH LOF did not alter *rh2-1* levels, but *rh2-2*, *rh2-3*, and *rh2-4* were all decreased, consistent with an endogenous role for TH signaling in regulating the distal members of the *rh2* array during juvenile zebrafish growth. Collectively, these results demonstrate that *rh2* opsin expression can be differentially regulated postembryonically, indicating that RH2 cones also remain plastic to the effects of TH. Further, the effects of TH appear to be dependent upon life history stage. For example, *rh2-2* was increased by T3 in larvae (Fig. 7B and D), but was unchanged by T4 in juveniles (Fig. 8B). We analyzed the *rh2* locus for putative TREs and RARE/RXREs (SI Appendix, SI Methods). Several of these elements were identified in the upstream regulatory regions of all 4 *rh2* genes (SI Appendix, Fig. S3B).

Additional Color Vision-Associated Transcripts Are Plastic to the Effects of TH. We next examined expression of the 2 remaining cone opsin transcripts in response to GOF and LOF of TH signaling, using

(LOF + T4) ($n = 7$) $P = 0.006$ compared to LOF. *lws2* abundance (C) in control ($n = 9$), is decreased by T4 GOF ($n = 9$) $P = 2.66\text{e-}06$ compared to control, increased in LOF ($n = 6$) $P = 4.38\text{e-}02$ compared to control, and decreased in Rescue ($n = 7$) $P = 3.61\text{e-}08$ compared to LOF. ddCT values were calculated by subtracting the dCT value for each fish from the average dCT values from the control fish in each experiment. *P* values were calculated by comparing the ddCT values for each fish from each condition using the Kruskal–Wallis test and the Conover post hoc test further adjusted by the Benjamini–Hochberg false-discovery rate method. Statistical notation: * $P < 0.05$, ** $P < 0.01$, **** $P < 0.0001$. (D–G) *lws::PAC(H)* whole-mounted retinas visualized by confocal microscopy of 31 dpf DMSO (control) (D), T4 (GOF) (E), athyroid (LOF) (F), and Rescue (LOF+T4) (G) juveniles. D, dorsal; N, nasal. Arrowhead in F indicates restricted ventral expression domain of *lws1* in athyroid juvenile retina. (H) Whole-mounted retina of an age-matched RARE:eYFP juvenile showing domain of RA signaling restricted to ventral retina (arrowhead), and matching the domain of GFP (*lws1*) expression in athyroid retinas (arrowhead in F) of juvenile fish. (I) High-magnification view of *lws::PAC(H)* retina showing GFP/RFP colabeling (opsin switching) in T4-treated juveniles (not the same retina pictured in E). Green arrowhead indicates a GFP⁺ cone. White arrowhead indicates a colabeled (GFP⁺/RFP⁺) cone. (Scale bar in D [applies to D–H], 100 μm; in I, 50 μm.)

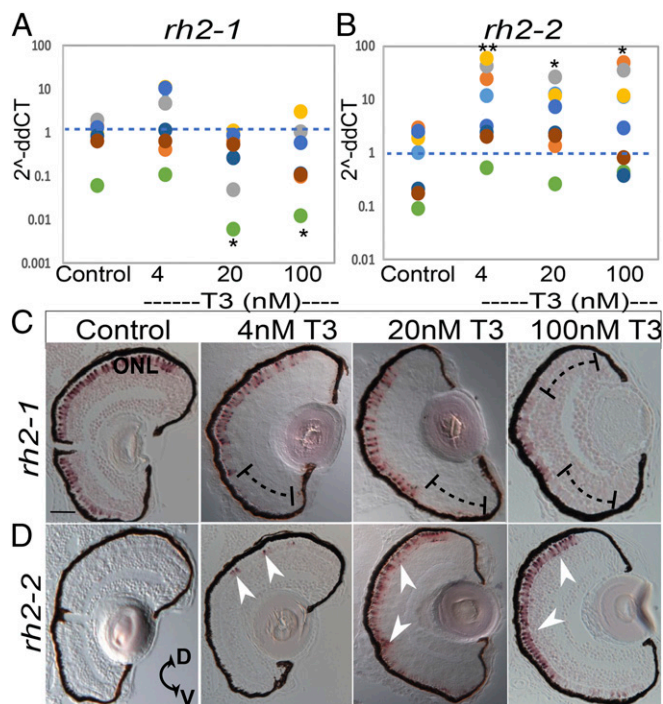


Fig. 7. qPCR and in situ hybridization for *rh2-1* and *rh2-2* gene expression reveals differential regulation after TH (T3) treatment from 2 to 4 dpf. (A and B) Scatter plots indicate fold-change abundance (2^{-ddCT}) of the indicated transcripts. Colors of dots correspond to separate experiments. Each dot represents 1 biological replicate (pooled RNA from ~5 larvae). *rh2-1* abundance (A) in DMSO control ($n = 7$), is unchanged by 4 nM T3 ($n = 7$) $P = 0.53$, decreased by 20 nM T3 ($n = 7$) $P = 0.0186$, and decreased by 100 nM T3 ($n = 7$) $P = 0.0259$. *rh2-2* abundance (B) in control ($n = 7$), is increased by 4 nM T3 ($n = 7$) $P = 0.0043$, increased by 20 nM T3 ($n = 7$) $P = 0.037$ and increased by 100 nM T3 ($n = 7$) $P = 0.026$. P values were calculated by comparing the ddCT values for treated vs. control from each experiment using the Kruskal–Wallis test and the Conover post hoc test further adjusted by the Benjamini–Hochberg false-discovery rate method. Statistical notation: * $P < 0.05$, ** $P < 0.01$. (C and D) In situ hybridization of cryosectioned eyes using gene specific probes for *rh2-1* (C) and *rh2-2* (D) from larvae treated 2 to 4 dpf with DMSO (control) or T3. Brackets in C indicate regions showing reduced expression domain of *rh2-1* due to T3 treatment; arrowheads in D indicate regions showing induced and expanded expression domain of *rh2-2* due to T3 treatment. D, dorsal; V, ventral. (Scale bar, 50 μm .)

the experimental design shown in Fig. 6A. In juveniles treated with T4 (GOF), *sws1* (*UV opsin*) transcript abundance was reduced by 2-fold, compared to controls (SI Appendix, Fig. S5A), and *sws2* (*blue opsin*) was reduced by 2.6-fold (SI Appendix, Fig. S5B), suggesting that exogenous TH can regulate all cone opsin genes in the zebrafish, regardless of whether they are tandemly replicated. However, in athyroid juveniles (LOF), *sws1* and *sws2* levels were not different compared to controls (SI Appendix, Fig. S5A and B), findings which are not consistent with endogenous functions for TH signaling in regulation of these genes in juvenile zebrafish.

Exogenous TH promotes the expression of the *cyp27c1* gene in adult zebrafish, within the retinal pigmented epithelium (33). *cyp27c1* encodes an enzyme that catalyzes the conversion of the A1 type chromophore (11-*cis* retinal) to an A2 type chromophore (11-*cis* dihydroretinal) (33). This change in chromophore causes a red shift in spectral sensitivity of the associated visual pigment (34). We confirmed that TH also up-regulates *cyp27c1* in juvenile zebrafish. In 2 of 4 biological replicates analyzed, *cyp27c1* transcript was not detected in controls, but was in the other 2 (SI Appendix, Table S2). In all replicates treated with T4, *cyp27c1* was detected, and at lower cycle thresholds (CTs) than the corresponding controls (where this comparison was possible)

(SI Appendix, Table S2), indicating that T4 increased *cyp27c1* transcript levels in the eyes of juvenile zebrafish.

Recently, it was reported that the transcription factor Six7 is required for *rh2* opsin expression in zebrafish (35, 36), and we reasoned that Six7 may be involved in the regulation of *rh2* genes in response to TH signaling. In juveniles treated with T4 (GOF), levels of *six7* transcript were slightly reduced, by 1.73-fold compared to controls (SI Appendix, Fig. S5C). Regulation of *six7* therefore could be downstream of TH signaling, suggesting an indirect mechanism for regulation of the *rh2* array by TH. However, in athyroid juveniles (LOF), *six7* was unchanged, compared to controls (SI Appendix, Fig. S5C), suggesting that endogenous TH signaling is not necessary to promote expression of *six7*, and supporting independent roles for this transcription factor and TH in the regulation of the *rh2* opsin genes.

Discussion

Regulation of differential expression of tandemly replicated opsin genes has been of high interest for decades (3, 4, 7), as these

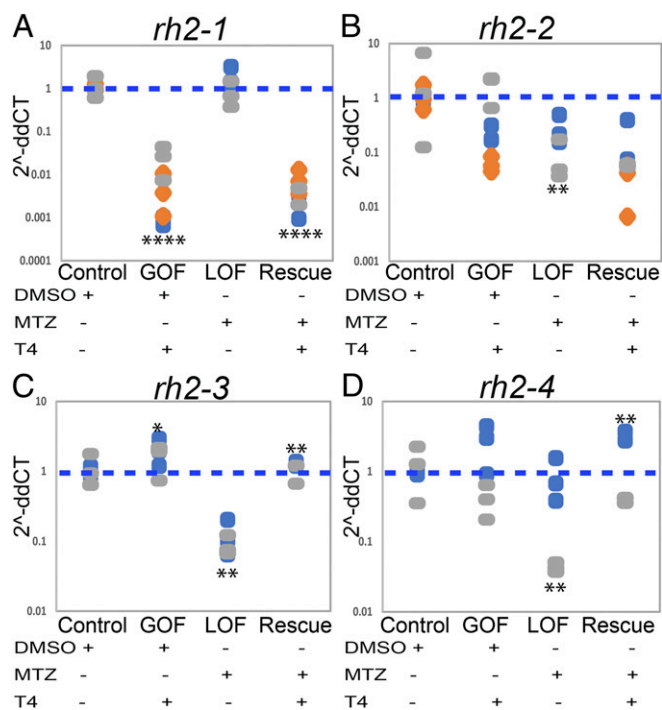


Fig. 8. Plasticity of *rh2* differential expression by TH (T4) in normal and athyroid juveniles. All panels show qPCR measuring *rh2* abundance. Scatter plots indicate fold-change in abundance (2^{-ddCT}) of the indicated transcripts. Colors indicate separate experiments. Each marker represents an individual fish. (A) *rh2-1* abundance in DMSO (control) ($n = 9$), is reduced by T4 (GOF) ($n = 9$) $P = 0.000002$, not changed in metronidazole (athyroid; LOF) ($n = 6$) $P = 0.88$ and reduced in Rescue (LOF+T4) ($n = 7$) in comparison to LOF $P = 0.000003$. (B) *rh2-2* abundance in control ($n = 9$), is unchanged by T4 GOF ($n = 9$) $P = 0.052$ compared to control, reduced in LOF ($n = 6$) $P = 0.0098$ compared to control, and unchanged in Rescue ($n = 7$) $P = 0.28$ compared to LOF. (C) *rh2-3* in control ($n = 6$), is increased by T4 GOF ($n = 6$) $P = 0.022$, decreased in LOF ($n = 6$) $P = 0.0023$ in comparison with control, and increased in Rescue ($n = 4$) $P = 0.0015$ compared to LOF. (D) *rh2-4* in control ($n = 6$), is not changed by T4 GOF ($n = 6$) $P = 0.799$ compared to control, decreased in LOF ($n = 4$) $P = 0.0035$ compared to control, and increased in Rescue ($n = 4$) $P = 0.0055$ compared to LOF. ddCT values were calculated by subtracting the dCT value for each fish from the average dCT values from the control fish in each experiment. P values were calculated by comparing the ddCT values for each fish from each condition using the Kruskal–Wallis test and the Conover post hoc test further adjusted by the Benjamini–Hochberg false-discovery rate method. Statistical notation: * $P < 0.05$, ** $P < 0.01$, **** $P < 0.0001$.

replications provided the raw genetic material for the evolution of trichromatic color vision in primates, and diversification of visually mediated behaviors in primates (37, 38) and fish (6, 7). However, in order for replicated opsin genes to contribute to multichromatic color vision, the replicates must be both spectrally divergent and expressed in distinct cone populations (6). Our previous study revealed that a transacting paracrine signal, RA, regulates differential expression of the tandemly duplicated *lws* array in zebrafish (10). In the present study we demonstrate that: 1) the endocrine signal, TH, is a relatively more potent regulator of the *lws* array; 2) TH can also regulate expression from the tandemly quadruplicated *rh2* array; and 3) TH is an endogenous regulator of both arrays, likely causing individual cones to switch opsins and change their peak spectral sensitivities as the zebrafish grows. We also reveal striking plasticity of LWS and RH2 cones to differentially express members of the tandem arrays in response to TH manipulations during juvenile growth.

TH has been demonstrated to regulate photoreceptor differentiation, cone survival, and expression of specific opsin genes, in retinal cell cultures and in vivo. For example, addition of T3 to cultured embryonic rat retinal cells (16), or to fetal human retinal cells (17), promotes progenitor cell survival and differentiation into cones. In addition, an extensive body of work from many investigators has illuminated roles for TH in mammalian systems in promoting expression of the MWS/LWS cone at the expense of the SWS opsin. Mice treated with T3 show reduced SWS opsin and increased MWS opsin, disrupting the endogenous dorsal-ventral gradient of MWS to SWS (15). Correspondingly, pharmacological suppression of serum TH in adult mice and rats results in increased SWS opsin and reduced MWS opsin, and the normal pattern of opsin expression and distribution can be restored in athyroid mice by TH treatment (39). Recently Eldred et al. (23) reported that retinal organoids differentiated from human induced pluripotent stem cells also respond to T3, by increasing expression of MWS/LWS opsin while reducing expression of SWS opsin, and this mirrors an endogenous temporal regulatory pattern of human opsin expression (40). In teleost fish, the majority of studies have focused upon roles for TH in regulation of the SWS opsins, *Sws1* (UV opsin) and *Sws2* (blue opsin). In salmonids, TH signaling accelerates opsin expression during photoreceptor differentiation and induces a switch from *sws1* to *sws2* expression in differentiated cones (18). Similarly, TH treatment of rainbow trout reduces expression of *sws1* (41). We add to this body of knowledge an additional endogenous function for TH, in regulating differential expression of opsin genes residing upon tandemly replicated arrays, and acting as a mechanism for the spatiotemporal control of their expression. We speculate that TH was evolutionarily co-opted for this function as tandemly replicated opsin genes became subfunctionalized, diverging in peak spectral sensitivities of the encoded opsin proteins. Although spatiotemporal gradients of TH signaling have not been demonstrated in zebrafish, several other vertebrates show pronounced dorsal-ventral gradients of T3 or its deiodinase regulatory enzymes [mouse (15); *Xenopus* (42); chick (13)]. Specifically in the chick, TH signaling components, including the TH receptors TR α and TR β , as well as the deiodinases Dio2 and Dio3, are expressed in the developing retina in 3 sequential, spatially stereotyped waves that coincide with neurogenesis, cell differentiation, and loss of progenitors (13).

We observed that in athyroid juveniles, *lws1* expression was still detected in ventral retina (Fig. 6F), a region that coincides with an RA signaling domain in age-matched *RARE:YFP* transgenic fish (Fig. 6H). The expansion of the *lws1* expression domain is therefore dependent upon TH signaling, but RA signaling is likely sufficient for inducing and maintaining the ventral expression domain. Putative TREs/RAREs/RXREs are predicted in the regulatory regions upstream of the *lws* genes (SI Appendix, Fig. S4A), consistent with this interpretation. Predicted TREs and RAREs are located within the essential regulatory region LAR (SI Appendix, Fig. S4A), which functions as an enhancer of either *lws* gene but does not contain elements necessary for determining

spatiotemporally accurate expression (8). The LAR is hypothesized to interact with sequences that are predicted to reside in other regions of the *lws* locus in order to determine cell-specific expression (8). The putative TREs/RAREs/RXREs residing in these regions outside of the LAR may facilitate this interaction. In contrast, the LCR of the *rh2* locus does contain the necessary elements to determine cell-specific and spatially accurate expression of the *rh2* genes in adult zebrafish (11). It has been demonstrated that expression from the *rh2* opsin gene array in adult zebrafish is dependent on relative distance of the gene to the *rh2* LCR for the first 3 members, while *rh2-4* is insensitive to the distance effect (12). In addition, the proximal upstream regions of *rh2-1*, *rh2-2*, and *rh2-4*, but not *rh2-3*, are sufficient for specifying their respective expression domains in the retina (12). The putative TREs/RAREs/RXREs predicted in the upstream regulatory regions of all 4 members of the *rh2* array (SI Appendix, Fig. S4B) may participate in these regulatory interactions. It is interesting that the role of TH signaling appears distinctive in larvae vs. juvenile zebrafish. These life history-dependent differences may indicate that the *rh2* array, or some of its member genes, may be dependent upon factors other than TH. During the first month of zebrafish growth the *rh2* expression patterns, particularly that of *rh2-2*, undergo extensive and dynamic changes in their respective spatial domains (9). Analysis of the spatial changes in expression in response to changes in TH signaling, as well as dissection of the regulatory regions of the *rh2* and *lws* loci, together with TH manipulations, will help to reveal the elements necessary and sufficient for the response to TH.

The present work, and many previous, seminal studies, contribute to the current model for vertebrate cone determination, in which a series of transcription factors expressed in photoreceptor progenitors and precursors, including TR β 2, determines cone phenotype and importantly the type of opsin expressed (43). However, in case of the choice of opsin from a tandemly replicated array, the most recent model in the field has considered this choice a stochastic process leading to permanent expression of a specific opsin (4). Evidence supporting this model is limited, in part due to reliance upon model organisms, such as mouse, that do not have tandemly replicated opsins in their genomes. The zebrafish, with 2 tandemly replicated opsin arrays, has provided the means to test alternative hypotheses for their regulation. Together with our prior demonstration that the paracrine signal, RA, acts as an endogenous regulator of differential expression from the zebrafish *lws* array (10), the present study provides evidence that tandemly replicated opsin arrays are regulated by the endocrine signal, TH, and that the choice of opsin from each array is not always a permanent choice, but remains plastic to TH signaling during organism development and growth.

The responses of the zebrafish *lws* and *rh2* arrays to TH GOF and LOF are complex. In larvae treated with a relatively low dose of T3, the *lws1* transcript was increased in abundance but *lws2* was not changed. The *rh2-1* transcript was unchanged, but abundance of *rh2-2* transcript was increased. With higher concentrations of T3, *lws1* and *rh2-2* expression continues to be increased while *lws2* and *rh2-1* expression is decreased. This suggests that the expression from each array becomes biased toward the longer wavelength-sensitive opsins of the array by TH. TH in larvae promotes *lws1* over *lws2* [*Lws1* λ_{max} = 558 nm, *Lws2* λ_{max} = 548 nm (7)], and *rh2-2* and *rh2-3* over *rh2-1* [*Rh2-3* λ_{max} = 488 nm, *Rh2-4* λ_{max} = 505 nm, *Rh2-1* λ_{max} = 467 nm, *Rh2-2* λ_{max} = 476 nm (7)]. LOF in juveniles correspondingly suppresses *lws1*, *rh2-2*, *rh2-3*, and *rh2-4*. Together with the generally suppressive effects of TH on the *sws* opsin genes in zebrafish (present study), as well as in salmonids (18, 41) and mammals (15, 39), a conserved role for TH appears to be to promote visual changes that favor sensitivity to longer wavelengths of the electromagnetic spectrum. This shift in sensitivity may be further enhanced by a TH-mediated conversion of the A1 chromophore to A2 (31, 44) by the enzyme Cyp27c1, which is promoted by TH (ref. 33 and the present study). The chromatic organization of the larval zebrafish retina matches the chromatic features of the natural environment

and the behavioral requirements for feeding and avoiding predation (45). As zebrafish grow through the juvenile stage, feeding strategies change (46) in a TH-dependent manner (47), body pigmentation patterns of conspecifics change in a TH-dependent manner (29), shoaling behavior begins (48), mobility and use of the expanse of the water column increases (48), and new predators emerge (48). It is likely that the TH-mediated shifts in color vision over an animal's lifespan are important in adapting to such changing visual demands in coordination with other anatomical and physiological changes.

Materials and Methods

Animals. Zebrafish were maintained in monitored aquatic housing units on recirculating system water at 28.5 °C. Embryos were collected according to Westerfield (49), with light onset considered to be 0 h postfertilization (hpf) and embryonic age timed accordingly thereafter, with 24 hpf considered 1 dpf, 48 hpf considered 2 dpf, and so forth. Embryos used for whole-mount analyses were kept transparent by incubating them in system water containing 0.003% phenylthiourea (PTU) to inhibit melanin synthesis. All experiments using animals were approved by the University of Idaho's Animal Care and Use Committee. Wild-type embryos were of an in-house outbred strain originally obtained from Scientific Hatcheries (now Aquatica Tropicals) and are referred to as "wild type." In the transgenic line *Tg(LWS1/GFP-LWS2/RFP-PAC(H)) #430*, the "transgene" consists of a PAC clone in which the first exons of *lws1* and *lws2* were replaced with GFP and RFP, respectively, each followed by a polyadenylation sequence (8). The spatiotemporal expression patterns of GFP and RFP replicate endogenous patterns of *lws1* and *lws2*. We refer to this line as *lws:PAC(H)*. The transgenic zebrafish line "Ligand Trap-Thyroid Receptor β " (LT-TR β) was a generous gift from Jens Tiefenbach, InDanio Bioscience Inc., Toronto, ON, Canada. In the ligand trap (LT) system, a Lex-DNA binding domain (DBD) human nuclear receptor ligand-binding domain (LBD) fusion protein is used to signal the presence of ligand in vivo. Binding of the fusion protein to a Lex-dependent GFP reporter results in GFP expression in the presence of endogenous or added ligands and cofactors. The LT-TR β line also has an element called LOOP. This element contains the Col1 binding sites for LEXDBD followed by a LEX-DBD-GAL activation domain. Therefore, an activated TR β will lead to reporter GFP expression but also to GAL activation domain expression, which will increase GFP expression (27). The transgenic line *Tg(tg:nVenus-2a-nfsB)wp.rt8* was a generous gift from David Parichy, University of Virginia, Charlottesville, VA. The transgene consists of the thyroglobulin start site driving expression of nuclear Venus linked to the 2A viral peptide and nitroreductase encoded by *nfsB* (29). The transgenic zebrafish line RGNy was generously provided by Elwood Linney, Duke University School of Medicine, Durham, NC. The transgene consists of 3 copies of RAREs derived from the mouse RAR β gene, a zebrafish basal promoter, a Topaz YFP sequence, an SV40 polyadenylation signal, and a small t intron. The endogenous expression patterns of YFP in these fish are consistent with known areas undergoing RA signaling and YFP reporter expression increases in response to exogenous RA (32, 50). We refer to this line as *RARE:YFP*.

T3/T4 and Metronidazole Treatments and Heat Shock. Stock solutions of T3 and metronidazole were prepared in DMSO (Sigma) and stored in the dark at -20 °C. Prior to treatment, embryos/larvae were manually dechorionated, and then 1,000 \times stock solution was added to the water to result in the final concentrations indicated in *Results* (DMSO was at a final concentration of 0.1%). T3 was used as the experimental treatment for embryos/larvae, because T3 treatment was shown to result in T3 accumulation within the eyes of embryonic zebrafish to a greater extent than did a T4 treatment (27). T3-treated larvae did not appear grossly different from controls, except for a lack of pigmentation. The appearance of athyroid juveniles was similar to that reported by McMenamain et al. (29). T4 stock solutions were prepared in NaOH and stored in the dark at -20 °C. Juveniles were maintained in 250-mL beakers in system water. Next, 1,000 \times stock T4 solution was added to the water to result in the final concentrations indicated in *Results* (NaOH was at a final concentration of 0.01%). T4 was used as the experimental treatment for juveniles, because T4 must travel to target tissues via the circulation at this stage, and to be consistent with other studies of TH treatment in postlarval fish (29, 33, 44). T4 treatments had no noticeable effect on the general appearance of juveniles. For treatments lasting longer than 1 d, solutions were refreshed every 24 h. Heat shocks (to induce expression of "Ligand Trap") were performed at 2 or 3 dpf by transferring embryos to 37 °C for 30 min.

qRT-PCR Analysis. Total RNA from each treatment group of pooled (5, 6) whole larvae or in the case of juveniles, total RNA from the 2 eyes of each fish from each condition, was extracted using the Machery-Nagel kit and was used to synthesize cDNA template using the High Capacity cDNA Reverse Transcription kit with random primers (Applied Biosystems). Gene-specific primer pairs are listed in *SI Appendix, Table S3*. Amplification to measure abundance of specific transcripts was performed on a model 7900HT Fast Real-Time PCR System using SYBR-Green PCR Master Mix (Applied Biosystems). Relative quantitation of gene expression using the ddCT method (Applied Biosystems-Guide to Performing Relative Quantitation of Gene Expression Using Real-Time Quantitative PCR) between control and experimental treatments was determined using the 18s ribosomal RNA and β -actin as the endogenous references. Graphing and statistics were performed using Excel. *P* values were calculated using a Wilcoxon Mann-Whitney *U* test, or the Kruskal-Wallis Test with a Conover post hoc test further adjusted by the Benjamini-Hochberg false-discovery rate method.

Histological Processing and In Situ Hybridization. Fixation and preparation of embryos for tissue sectioning and in situ hybridization were performed as previously described (50, 51). For in situ experiments, cRNA probes were generated by in vitro reverse transcription of cDNAs. Digoxigenin- (dig-) UTPs were incorporated into probes for detection with anti-dig antibodies conjugated to alkaline phosphatase and visualized with NBT-BCIP substrate. Images were captured using a Leica DM2500 compound microscope with a Leica DFC700T camera system. In situs were viewed and photographed using Nomarski (differential interference contrast) optics and brightfield optics.

Confocal Photography and Quantification: *lws:PAC(H)* Embryos. *lws:PAC(H)* embryos were maintained in system water with PTU starting at 24 hpf. At 2 or 3 dpf, embryos were treated with T3 or DMSO through 3 or 4 dpf, and then fixed in 4% paraformaldehyde in phosphate-buffered (pH = 7.0) 5% sucrose solution for 1 h, washed once in phosphate-buffered sucrose solution for 30 min, followed by 3 washes in PBS. Following fixation and washing, embryos were incubated in PBS at 4 °C in the dark for no longer than 24 h. Immediately prior to imaging, whole eyes were removed from fixed embryos, the sclera teased away by microdissection, and eyes were then coverslipped in glycerol. Imaging was performed with a 20 \times dry or 40 \times water-immersion lens using a Nikon Andor spinning-disk confocal microscope equipped with a Zyla sCMOS camera running Nikon Elements software. A z-series covering the entire globe of the eye was obtained with 3- μ m step sizes. FIJI (ImageJ) was used to flatten z-stacks via max projection and adjust brightness/contrast. Images from samples where GFP signal was not resolvable in all planes (due to the developing RPE and iridophores in residual sclera) were excluded from analysis.

Confocal Photography: Juvenile Zebrafish Retinal Whole Mounts. One-month-old juvenile zebrafish were anesthetized and decapitated. Heads were fixed in 4% paraformaldehyde/sucrose solution as described above for 30 min. After 30 min, heads were removed and corneas punctured with a dissecting pin, then returned to the fixation solution for another 30 min. The lens was removed followed by the whole retina. The retina was flattened and mounted in glycerol and coverslipped. Imaging was performed at 20 \times (dry) magnification using a Nikon Andor spinning-disk confocal microscope equipped with a Zyla sCMOS camera running Nikon Elements software. A z-series covering the entire retina was obtained with 3- μ m step sizes. The stitching feature was used to capture the whole retina. FIJI (ImageJ) was used to flatten z-stacks via maximum projection and adjust brightness/contrast.

Confocal Microscopy: Live Imaging. Five days postfertilization *lws:PAC(H)* larvae were immersed in 100 nM T3 at 8:00 AM. Before imaging, larvae were immobilized in a 2% agarose pad in a 35-mm glass-bottom dish and overlaid with 28 °C system water containing 100 nM T3, 0.02% MS-222, and 0.003% PTU. Imaging was performed with a 40 \times water-immersion lens using a Nikon Andor spinning-disk confocal microscope equipped with a Zyla sCMOS camera running Nikon Elements software. Time course began at 4:00 PM and lasted for 9 h total. Images were captured at 30-min intervals. A 3- μ m step z-series covering the area of interest was converted into volume view using the Nikon Elements software. The Director feature in Nikon Elements software was used to create the time-lapse movie (Movie S1).

ACKNOWLEDGMENTS. The authors thank Dr. Jens Tiefenbach for the gift of the T3 "ligand trap" transgenic line; Dr. Rachel Wong for the *tr β :tdTomato* transgenic line; Dr. David Parichy for the *Tg(tg:nVenus-2a-nfsB)^{wp.rt8}* transgenic line; Dr. Elwood Linney for the *RARE:YFP* transgenic line; Dr. Thomas Euler

for providing the WinDRP program; Ms. Ann Norton of the University of Idaho Optical Imaging Core; Jaclyn Huffman and Kiah Stewart of the University of Idaho Laboratory Animal Research Facility; and Lindsey Leadbetter of the D.L.S. laboratory for technical assistance. This work was supported by NIH Grants R01 EY012146 (to D.L.S.) and R01 EY012146-16S1 (to D.L.S. and A.A.F.); The Malcolm and Carol Renfrew Faculty Fellowship (D.L.S.); National

Science Foundation REU Site 146096 (to C.G.); project support funds available through the University of Idaho Institute for Bioinformatics and Evolutionary Studies (NIH P30 GM103324) and Idaho INBRE (NIH P20 GM103408); and the Japan Society for the Promotion of Science Grant 18H04005 (to S.K.). NIH Grant S10 OD0108044 (to D.L.S.) funded the purchase of the Nikon/Andor spinning-disk confocal microscope and camera.

- S. Yokoyama, Molecular evolution of vertebrate visual pigments. *Prog. Retin. Eye Res.* **19**, 385–419 (2000).
- J. Nathans, D. Thomas, D. S. Hogness, Molecular genetics of human color vision: The genes encoding blue, green, and red pigments. *Science* **232**, 193–202 (1986).
- D. Vollrath, J. Nathans, R. W. Davis, Tandem array of human visual pigment genes at Xq28. *Science* **240**, 1669–1672 (1988).
- Y. Wang *et al.*, Mutually exclusive expression of human red and green visual pigment-reporter transgenes occurs at high frequency in murine cone photoreceptors. *Proc. Natl. Acad. Sci. U.S.A.* **96**, 5251–5256 (1999).
- J. A. Kuchenbecker, M. Sahay, D. M. Tait, M. Neitz, J. Neitz, Topography of the long- to middle-wavelength sensitive cone ratio in the human retina assessed with a wide-field color multifocal electroretinogram. *Vis. Neurosci.* **25**, 301–306 (2008).
- C. M. Hofmann, K. L. Carleton, Gene duplication and differential gene expression play an important role in the diversification of visual pigments in fish. *Integr. Comp. Biol.* **49**, 630–643 (2009).
- A. Chinen, T. Hamaoka, Y. Yamada, S. Kawamura, Gene duplication and spectral diversification of cone visual pigments of zebrafish. *Genetics* **163**, 663–675 (2003).
- T. Tsujimura, T. Hosoya, S. Kawamura, A single enhancer regulating the differential expression of duplicated red-sensitive opsin genes in zebrafish. *PLoS Genet.* **6**, e1001245 (2010).
- M. Takechi, S. Kawamura, Temporal and spatial changes in the expression pattern of multiple red and green subtype opsin genes during zebrafish development. *J. Exp. Biol.* **208**, 1337–1345 (2005).
- D. M. Mitchell *et al.*, Retinoic acid signaling regulates differential expression of the tandemly-duplicated long wavelength-sensitive cone opsin genes in zebrafish. *PLoS Genet.* **11**, e1005483 (2015).
- T. Tsujimura, A. Chinen, S. Kawamura, Identification of a locus control region for quadruplicated green-sensitive opsin genes in zebrafish. *Proc. Natl. Acad. Sci. U.S.A.* **104**, 12813–12818 (2007).
- T. Tsujimura, R. Masuda, R. Ashino, S. Kawamura, Spatially differentiated expression of quadruplicated green-sensitive RH2 opsin genes in zebrafish is determined by proximal regulatory regions and gene order to the locus control region. *BMC Genet.* **16**, 130 (2015).
- J. M. Trimarchi, S. Harpavat, N. A. Billings, C. L. Cepko, Thyroid hormone components are expressed in three sequential waves during development of the chick retina. *BMC Dev. Biol.* **8**, 101 (2008).
- A. M. Houbrechts *et al.*, Deiodinase knockdown affects zebrafish eye development at the level of gene expression, morphology and function. *Mol. Cell. Endocrinol.* **424**, 81–93 (2016).
- M. R. Roberts, M. Srinivas, D. Forrest, G. Morreale de Escobar, T. A. Reh, Making the gradient: Thyroid hormone regulates cone opsin expression in the developing mouse retina. *Proc. Natl. Acad. Sci. U.S.A.* **103**, 6218–6223 (2006).
- M. W. Kelley, J. K. Turner, T. A. Reh, Ligands of steroid/thyroid receptors induce cone photoreceptors in vertebrate retina. *Development* **121**, 3777–3785 (1995).
- M. W. Kelley, J. K. Turner, T. A. Reh, Regulation of proliferation and photoreceptor differentiation in fetal human retinal cell cultures. *Invest. Ophthalmol. Vis. Sci.* **36**, 1280–1289 (1995).
- K. J. Gan, I. Novales Flamarique, Thyroid hormone accelerates opsin expression during early photoreceptor differentiation and induces opsin switching in differentiated TR α -expressing cones of the salmonid retina. *Dev. Dyn.* **239**, 2700–2713 (2010).
- A. C. Bianco, P. R. Larsen, Cellular and structural biology of the deiodinases. *Thyroid* **15**, 777–786 (2005).
- M. R. Roberts, A. Hendrickson, C. R. McGuire, T. A. Reh, Retinoid X receptor (γ) is necessary to establish the S-opsin gradient in cone photoreceptors of the developing mouse retina. *Invest. Ophthalmol. Vis. Sci.* **46**, 2897–2904 (2005).
- L. Ng *et al.*, A thyroid hormone receptor that is required for the development of green cone photoreceptors. *Nat. Genet.* **27**, 94–98 (2001).
- Y. Fei, T. E. Hughes, Transgenic expression of the jellyfish green fluorescent protein in the cone photoreceptors of the mouse. *Vis. Neurosci.* **18**, 615–623 (2001).
- K. C. Eldred *et al.*, Thyroid hormone signaling specifies cone subtypes in human retinal organoids. *Science* **362**, eaau6348 (2018).
- J. E. Cook, Spatial properties of retinal mosaics: An empirical evaluation of some existing measures. *Vis. Neurosci.* **13**, 15–30 (1996).
- R. W. Rodieck, The density recovery profile: A method for the analysis of points in the plane applicable to retinal studies. *Vis. Neurosci.* **6**, 95–111 (1991).
- S. C. Suzuki *et al.*, Cone photoreceptor types in zebrafish are generated by symmetric terminal divisions of dedicated precursors. *Proc. Natl. Acad. Sci. U.S.A.* **110**, 15109–15114 (2013).
- J. Tiefenbach *et al.*, A live zebrafish-based screening system for human nuclear receptor ligand and cofactor discovery. *PLoS One* **5**, e9797 (2010).
- J. Tiefenbach *et al.*, Idebenone and coenzyme Q₁₀ are novel PPAR α/γ ligands, with potential for treatment of fatty liver diseases. *Dis. Model. Mech.* **11**, dmm034801 (2018).
- S. K. McMenamin *et al.*, Thyroid hormone-dependent adult pigment cell lineage and pattern in zebrafish. *Science* **345**, 1358–1361 (2014).
- J. Chang *et al.*, Changes in thyroid hormone levels during zebrafish development. *Zool. Sci.* **29**, 181–184 (2012).
- T. Suliman, I. Novales Flamarique, Visual pigments and opsin expression in the juveniles of three species of fish (rainbow trout, zebrafish, and killifish) following prolonged exposure to thyroid hormone or retinoic acid. *J. Comp. Neurol.* **522**, 98–117 (2014).
- A. Perz-Edwards, N. L. Hardison, E. Linney, Retinoic acid-mediated gene expression in transgenic reporter zebrafish. *Dev. Biol.* **229**, 89–101 (2001).
- J. M. Enright *et al.*, Cyp27c1 red-shifts the spectral sensitivity of photoreceptors by converting vitamin A(1) into A(2). *Curr. Biol.* **25**, 3048–3057 (2015).
- G. Wald, The porphyropsin visual system. *J. Gen. Physiol.* **22**, 775–794 (1939).
- Y. Ogawa, T. Shiraki, D. Kojima, Y. Fukada, Homeobox transcription factor Six7 governs expression of green opsin genes in zebrafish. *Proc. Biol. Sci.* **282**, 20150659 (2015).
- M. Sotolongo-Lopez, K. Alvarez-Delfin, C. J. Saade, D. L. Vera, J. M. Fadool, Genetic dissection of dual roles for the transcription factor six7 in photoreceptor development and patterning in zebrafish. *PLoS Genet.* **12**, e1005968 (2016).
- P. W. Lucas, B. W. Darvell, P. K. D. Lee, T. D. B. Yuen, M. F. Choong, Colour cues for leaf food selection by long-tailed macaques (*Macaca fascicularis*) with a new suggestion for the evolution of trichromatic colour vision. *Folia Primatol. (Basel)* **69**, 139–152 (1998).
- Y. Matsumoto *et al.*, Evolutionary renovation of L/M opsin polymorphism confers a fruit discrimination advantage to ateline New World monkeys. *Mol. Ecol.* **23**, 1799–1812 (2014).
- A. Glaschke *et al.*, Thyroid hormone controls cone opsin expression in the retina of adult rodents. *J. Neurosci.* **31**, 4844–4851 (2011).
- K. M. O'Brien, D. Schulte, A. E. Hendrickson, Expression of photoreceptor-associated molecules during human fetal eye development. *Mol. Vis.* **9**, 401–409 (2003).
- J. C. Raine, C. W. Hawryshyn, Changes in thyroid hormone reception precede SW51 opsin downregulation in trout retina. *J. Exp. Biol.* **212**, 2781–2788 (2009).
- N. Marsh-Armstrong, H. Huang, B. F. Remo, T. T. Liu, D. D. Brown, Asymmetric growth and development of the *Xenopus laevis* retina during metamorphosis is controlled by type III deiodinase. *Neuron* **24**, 871–878 (1999).
- D. Forrest, A. Swaroop, Minireview: The role of nuclear receptors in photoreceptor differentiation and disease. *Mol. Endocrinol.* **26**, 905–915 (2012).
- W. T. Allison, T. J. Haimberger, C. W. Hawryshyn, S. E. Temple, Visual pigment composition in zebrafish: Evidence for a rhodopsin-porphyrin interchange system. *Vis. Neurosci.* **21**, 945–952 (2004).
- M. J. Y. Zimmermann *et al.*, Zebrafish differentially process color across visual space to match natural scenes. *Curr. Biol.* **28**, 2018–2032.e5 (2018).
- R. E. Westphal, D. M. O'Malley, Fusion of locomotor maneuvers, and improving sensory capabilities, give rise to the flexible homing strikes of juvenile zebrafish. *Front. Neural Circuits* **7**, 108 (2013).
- S. McMenamin, C. Carter, W. J. Cooper, Thyroid hormone stimulates the onset of adult feeding kinematics in zebrafish. *Zebrafish* **14**, 517–525 (2017).
- R. E. Engeszer, L. B. Patterson, A. A. Rao, D. M. Parichy, Zebrafish in the wild: A review of natural history and new notes from the field. *Zebrafish* **4**, 21–40 (2007).
- M. Westerfield, *The Zebrafish Book. A Guide for the Laboratory Use of Zebrafish (Danio rerio)* (University of Oregon Press, 2000), vol. **385**.
- C. B. Stevens, D. A. Cameron, D. L. Stenkamp, Plasticity of photoreceptor-generating retinal progenitors revealed by prolonged retinoic acid exposure. *BMC Dev. Biol.* **11**, 51 (2011).
- D. L. Stenkamp, R. A. Frey, D. E. Mallory, E. E. Shupe, Embryonic retinal gene expression in sonic-you mutant zebrafish. *Dev. Dyn.* **225**, 344–350 (2002).